PAPER • **OPEN ACCESS**

Pre-failure deformation monitoring as rockfall prediction tool

To cite this article: Miloš Marjanovi *et al* 2021 *IOP Conf. Ser.: Earth Environ. Sci.* **833** 012197

Pre-failure deformation monitoring as rockfall prediction tool

Miloš Marjanović[1], Biljana Abolmasov[1], Zoran Berisavljević[1], Marko Pejić[2], and Petko Vranić[2]

[1]University of Belgrade, Faculty of Mining and Geology, Đušina 7, Belgrade, Serbia

[2]University of Belgrade, Faculty of Civil Engineering, Bul. Kralja Aleksandra 73, Belgrade, Serbia

milos.marjanovic@rgf.bg.ac.rs

Abstract. In this article, we are elaborating an example of predictive rockfall assessment by using Terrestrial Laser Scanning (TLS) in monitoring a road cut, hosted in flysch rock formation, near Ljig in Serbia. A sequence of rockfall events from 2013-2019 is presented, while the cut has been more broadly investigated in our earlier work. Beside occasional rockfalls which are routinely detected by annual TLS monitoring, it was possible to track the pre-failure deformations preceding a series of rockfalls, reaching 0.3 m^3 in volume with 0.5 annual reoccurrence probability. Monitoring enabled identification of subtle displacements of about 1 cm after the first event in 2014 and keeping track of its progression. After a series of events in the following years, we were able to define the pre-failure threshold which can be applied to the adjacent rock blocks, assuming a similar block volume. It also enabled us to anticipate and simulate the event before it happens. This approach allows planning, prevention and protection, and there is a great deal of interest to standardize it for high-risk slopes and cuts in rock masses.

1. Introduction

Rockfalls are studied from various aspects and should be first observed from a wider, geo-structural and geomorphological context, which govern its local development. Studying of rockfalls primarily relies on historic data on their: spatial context; volume; frequency/return periods; runout and velocity. In practice, this is rarely as systematic as it should be, and data are usually scarce. Modeling and simulation is another tool that can be used to estimate some of the rockfall parameters and compensate for the lack of specific data [1]. Suspicious rock faces can be monitored for longer periods, using multiple monitoring systems (primarily Terrestrial Laser Scanning - TLS), seasonally or annually, or even in real-time. This provides systematic data for better understanding of the (pre)failure stages and allows for their linking with the triggering conditions. These precursory indicators are the subject of this research, which supports standardization of the monitoring practice in the rockfall management. One isolated rockfall example will be presented, while the entire rock slope will be analyzed in greater depth in the near future.

1.1. Related research

There is a substantial amount of scientific literature, papers, books, etc. related to the field of rock slope monitoring. In addition, commercial industries, especially consulting and monitoring instrument companies have numerous references and case studies completed in this field, sometimes failing to report ultimate findings, which might be very useful together with scientific publications. In this context

Figure 1. Location (left), appearance of the slope (middle), and plan of scanning disposition (right).

it is beyond the scope of this article to overview the current research and practice state-of-the-art in the field of LiDAR-based monitoring. Instead, some milestone contributions, after which our idea is inspired, will be briefly overviewed.

One of the pioneering reports in the rockfall-predictive context by Rosser et al. [2] describes not only the temporal and spatial changes of a rock face but uses precursory patterns to predict large rockfall events by a succession of small events. They confirmed indications from other rock cuts or steep cliffs investigations that frequency and rate of deformation of small events accelerates as the larger failure onsets. In addition, it is confirmed that the small events are spatially clustering around the future large failure scarp. They emphasize the importance of LiDAR scanning in further research and conclude that temporal resolution of the acquisition is its greatest drawback, especially for cross-correlation with the potential environmental triggers.

Similarly, Abellán et al. [3] emphasize the spatial, i.e. the pre-failure deformation aspect in their research, while acknowledging the frequency precursor analysis as impractical with TLS technique in their case. They emphasized site-specific limitations in respect to TLS monitoring. The cliff they monitored turned out to be very active, requiring more than twice-a-year field visits and provided cm displacements within two years of acquisition. They establish the detectable rockfall deformation threshold of 6 cm. They aligned with the Rosser et al. [2] methodology of comparing “zero”, i.e., the reference scan against each of the succeeding ones.

Kromer et al. [4] reported successful application using similar approach TLS acquisition for road corridors, but with doubled frequency and reduced point spacing resolution (10-20 cm), suggesting a systematic and quick tool for rockfall inventorying. However, they extended their analysis towards precursor indicators and increased the acquisition frequency after detecting a large part of one rock face with a massive tabular block slowly detaching. They managed to capture the acceleration stage of the rockslide and provided detailed analysis of pre-failure stages by comparing against numerous (weekly collected) sequences. They further emphasize the common errors originating from the line-of-sight referencing, i.e., using normal vector for detecting changes, and suggesting geometric corrections especially in oblique surfaces and steep slopes. Their principal finding is that smoothening of the point-cloud allows earlier detection of unstable blocks in comparison to raw cloud information.

De Vilder et al. [5] focused on scar/rock bridges analysis, therein combining TLS with high-definition photographs, suggesting that freshly detached rock bridges will seem more colorful and unweathered unlike joint surfaces or exposed facets. They combined pixel and point-cloud based processing algorithms to reveal fresh scars and rock bridges automatically, and then iteratively per each scanning/imaging sequence. Conveniently their strata resemble the flysch sequence we have been dealing with in our case study, so their experience was inspiring. They conclude that smaller events, do not leave clear footprints (scars, faces) as large events at specified scale, but seem better correlated to the external triggering factor, whereas larger events leave easily detectable footprints, but can occur independently from their actual driving agent as long as the rock bridge strength allows it under progressive failure assumption.

Janeras et al. [6] analyzed the famous Monserrat Mt. near Barcelona, by using different monitoring

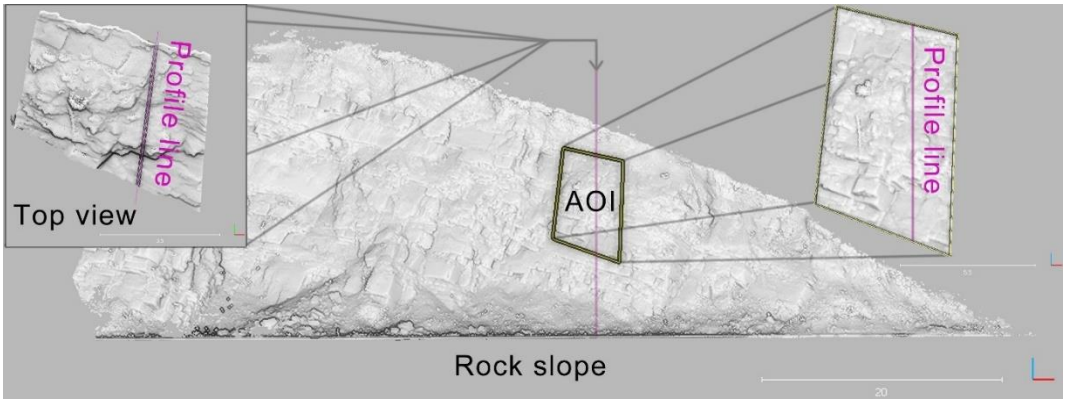

Figure 2. The 2013 point cloud, with sub-selected area of interest and predefined cross-section plane.

techniques. Their complex research had multiple objectives, targeted primarily towards measuring current and estimating future small/large scale rockfalls trends. Their principal finding in respect to our research is that TLS successfully captures cm displacements and can be used to anticipate the future events. In addition, mm displacements, are more oscillating in respect to temperature and other atmospheric agents, meaning that TLS can be fully used to monitor significant events.

Using all these experiences, we decided to improvise the referencing approach originally suggested by [2] and explore not only "zero" vs. current scanning sequence, but to explore differences between sequences as well. We also abandoned frequency analyses as impractical and focused on displacement analysis. We acknowledged the individuality of each rock face site and adopted the acquisition accordingly (annual) in respect to our study site. We tried to extract the deformation threshold as exampled in abovementioned case studies and estimate the total vectors instead of its line-of-sight component as suggested by [4].

2. Study site

Location of interest is positioned along IB22 highway, some 5 km to the south of the town of Ljig. It is a medium-sized rock slope, about 30 m high and 60 m long, with average slope of 60°, facing SSE (figure 1). It is a road cut engineered during 70's due to re-routing of an earlier flood-prone road. Opening this rock face resulted in intensive weathering and deformations related to the relaxation (tensile failures parallel to the face, small-scale shearing, etc.), causing relatively active slope. Rockfall volume and runout were considered as insignificant, and the slope is therefore, left unsupported and unprotected (figure 2). The cut seems to be composed of fresh rock, since their equivalents in the near-by tunnel, constructed in 2016-2019, were much more weathered and looser, with much poorer mechanical properties.

The strata follow an incomplete flysch succession (which spreads over vast areas) of thicker coarse to conglomeratic sandstone, alternating with a thin laminated marly siltstone, while claystone is likely lost in the sediment transport or missing for other reasons. Tectonics is not particularly pronounced at the site or in its vicinity, the formation has moderately gentle bedding (40-45°) that is dipping towards NNE. Jointing is relatively regular, so the entire rock is split into prismatic to tabular blocks.

The subject road cut has been elaborated in various aspects throughout the years as its monitoring, as a pilot site for a scientific project TR36009 (Project of Ministry of Education, Science and technological development of Serbia) started in 2011-12 and lasted until 2020. Prior to 2013, the scans were conducted by different equipment, with different features, but ever since, it has become entirely systematic. Slope kinematic potential and joint distribution were reported in [7,8]. One set of bedding (orientation 39/44°) and two conjugated joint sets (orientation 187/62° and 148/79°) were established, appointing to the block and wedge failure potential. Rock block size and volumes (0.5-2.7 m^3) were reported in [9], as well as the first monitoring results and the first rockfall analyses, wherein several detachment zones were distinguished. Further on, these zones were used in the latest published work

[10] as source areas, wherein the rockfall trajectories were simulated for various settings. The rock strata were also sampled for laboratory tests (unofficial data: UCS 80-100 MPa, Tensile strength 30-40 MPa, Bulk density 25 kN/m^3), some fresh surfaces were scanned from close-range for potential roughness analyses, but this will be the subject of a detailed, compiled paper about this site. Further details are available in the above-listed contributions.

3. Materials and methods

Data acquisition and processing were conducted for relatively long period, including first couple of years of pilot work, and a systematic procedure was adopted and iterated.

3.1. TLS

Acquisition technique primarily involves direct time of flight (DTOF) TLS scanner Leica Scan Station P20. With the latest firmware upgrade, this model remains one of the most reliable and efficient scanners collecting million points per second and range of up to 100-120 m in optimal conditions. The laser beam width of 2.6 mm provides sub cm resolution at specified range, but it is rarely required. As an active sensor it radiates the beam of monochromatic near-infrared domain through a system of mirrors that precisely record horizontal and vertical angles during emission and reception. By measuring the return time and assuming the constant wave velocity distance to reflected object is calculated and stored together with horizontal and vertical angle per each position. It can also detect reflectivity of the target point, as potentially valuable information in rock slope analysis (surface rock type, weathering degree water content might be correlated). These angular and distance measurements allow accurate reconstruction of each target point spatial coordinates (X,Y,Z) in respect to the optical center of the instrument (0,0,0), with an accuracy of a few millimeters. In result, it generates a discrete surface model consisting of millions of points called point clouds, referenced to a relative Euclidean coordinate system originating from the optical center of the instrument.

In addition to X,Y,Z and reflection intensity (I) information, it is possible to extract color information of each point. This scanner has such features, so each point in the cloud is provided with X,Y,Z,I,R,G,B information, but R,G,B values can be also collected by using external, High-Definition cameras to obtain better results.

3.2. Data acquisition

The first couple of years of the slope monitoring were experimental with unregular and not as systematic data acquisition. This period was used to establish standard protocol and decide on resolution, temporal frequency, timing, and other important acquisition features. Since 2013, after experimenting with various settings, the acquisition is standardized as follows:

- Acquisition frequency is annual (once a year) since it has been proven (based on early results in the period 2011-2013) that there is not enough activity on the slope to measure monthly or seasonal sequences (time epochs).
- Acquisition time should be early spring, on a cloudy but not rainy day, to provide constant light/reflectivity conditions between scanning epochs and to avoid vegetation screening.
- R,G,B values are not to be sequentially collected, as they may differ significantly between adjacent scans and time epochs due to change of lighting, and mislead to changes that have not actually occurred.
- Acquisition is to be carried out from three stations, which are sufficient to overcome shadows in the scanned data, but always similar (roughly located) three positions should be used. For reliable registration process of the three adjacent scans, 5-8 equally distributed black/white (B/W) targets should be placed across the slope and surrounding area.
- Scanning parameters should be set to 6.3 mm/10m to provide spatial resolution at least of 3 cm over the entire rock face.
- Scanning parameters should also include full 360°/270° field of view, to ensure reliable georeferencing between epochs, using surface matching algorithm.

In result, 2013 to 2019, i.e. seven scanning epochs were collected at the study site, following the above protocol.

3.3. Data processing

Acquisition protocol was followed by a processing protocol which comprised of:

- Data processing in Leica Cyclone software (target and surface matching registration, surface matching georeferencing relative to zero epoch, segmentation and cloud cleaning, unifying to 3cm spatial resolution).
- Using CloudCompare software plug-in CANUPO classifier [11] to clean rest of the vegetation points for each epoch.
- Comparing cloud-to-cloud difference between each succeeding scanning epoch and also vs. "zero" scan using CloudCompare software functionalities.

In this particular case, a medium-sized rockfall event was isolated for the analysis (figure 2) and accordingly sub-selected from the main cloud by using constant polygon for clipping all sequence point clouds and preserve geometry of the current area of interest. In addition, a constant vertical cross-sectional plane was applied in the same fashion to extract the slope profile for the sub-selected point cloud set, comprising of 7 point clouds (2013-2019).

4. Results and discussion

The results will be presented sequentially, mimicking the data flow and monitoring activity. However, total observation period 2013-2019 will be used as the ultimate reference, together with between-sequence comparisons. In all analyses, cloud-to-cloud absolute changes above 0.5 cm were considered significant and interpreted as displacement. It is likely that values below this 0.5 cm threshold are affected by scanning errors, presence of vegetation, and other noise, which is why this threshold is applied. For better visualization and understanding of displacement rate and dynamics all succeeding scans are compared against each other, as well as against the latest 2019 scan (figure 3-4). In addition, a vertical profile line was constructed to extract cross-sections from point clouds for each sequence at the same position and provide 2D impression (XZ) of the componential and total displacements. Profile line is placed across the most active part of the AOI selection near-perpendicular to slope in X-axis direction (figure 2).

Comparison between 2013 ("zero" epoch) and 2014 epoch (figure 3a) reveals severe activity highlighting the two top block detachments, each of about 1x1x0.5 m in size. Detachment occurs along one of the slope-forming joint sets (orientation 187/62°) that daylights locally across the slope. The tensile strength of arguably 30 MPa that holds the blocks in such daylighting setting is quite possibly much lower at the tip of the progressing joint. It is hard to define its indirect trigger, as it is more likely that it is a temporally conditioned failure under progressive failure mode. This mechanism can be adopted as representative for all other events within the sub-selected area of interest. The largest absolute difference between these two sequences is about 40 cm. Unfortunately, this sequence has no reliable predecessor point cloud, and its detachments could not be analyzed for precursors. Figure 4a reveals relatively large total 2013-2019 detachment, reaching a couple of cubic meters in volume, with mainly blocky material and eroded debris/talus. The largest X direction displacement is about 70 cm. In figure 5a, the profile line misses the most of the 2013-2014 event and reveals low activity.

Comparison between 2014-2015 epochs (figure 3b) is also significant, as it reveals yet another event, but this time in the lower section of the area, seemingly unrelated to progressive failure of the previous (2013-2014) zone. An even larger volume of about 3 cubic meters is missing and similar blocky failures apply as previously described. Total 2014-2019 detachment (figure 4b) is very similar as before in terms of extent, volume, and maximal displacement. The cross-section (figure 5b) this time successfully captures the event through the middle and suggests that there was detectable bulging deformation prior to detachment. The maximal displacement which might be included as precursor for the subsequent event is 0.7663-0.7567 = 0.0096 m ≈ 1 cm (figure 5a-b).

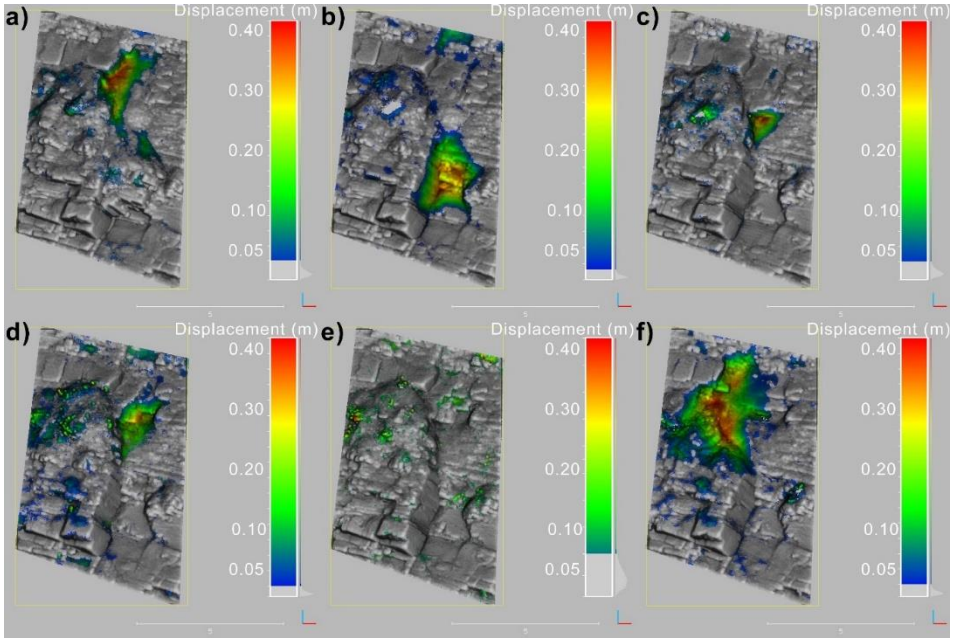

Figure 3. Cloud difference: a) 2013-14; b) 2014-15; c) 2015-16; d) 2016-17; e) 2017-18; f) 2018-19.

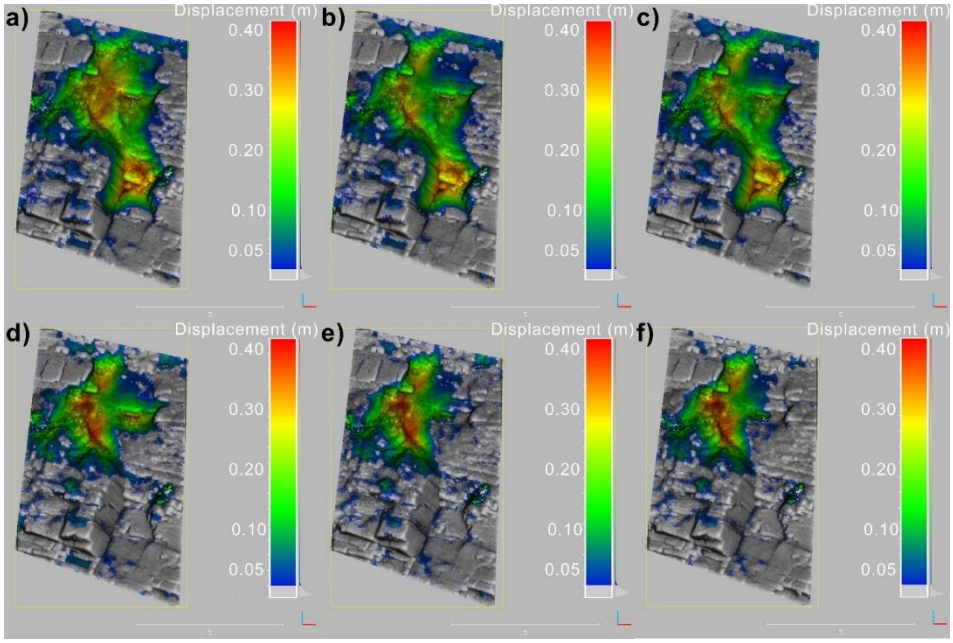

Figure 4. Cloud difference: a) 2013-19; b) 2014-19; c) 2015-19; d) 2016-19 e) 2017-19; f) 2018-19.

Comparison between 2015-2016 epoch (figure 3c) shows reduced activity but appoints to the zone which is somewhere in between the first two events, thereby supporting a progressive failure premise. Detached triangular block is about 0.3 m^3 in volume. Maximal X component displacement reaches about 40 cm. There is only subtle difference in respect of the total detachment (2015-2019), meaning that this event contributes very little in that respect. The cross-section successfully captures this event, but there were no detectable precursors, given the previous (2014-2015) large disturbance in slope geometry that have enclosed the extents of this event.

Comparison between 2016-2017 epoch (figure 3d) indicates further progressive block failures, in upslope direction. This feature will become interesting for precursor analysis in the following sequences.

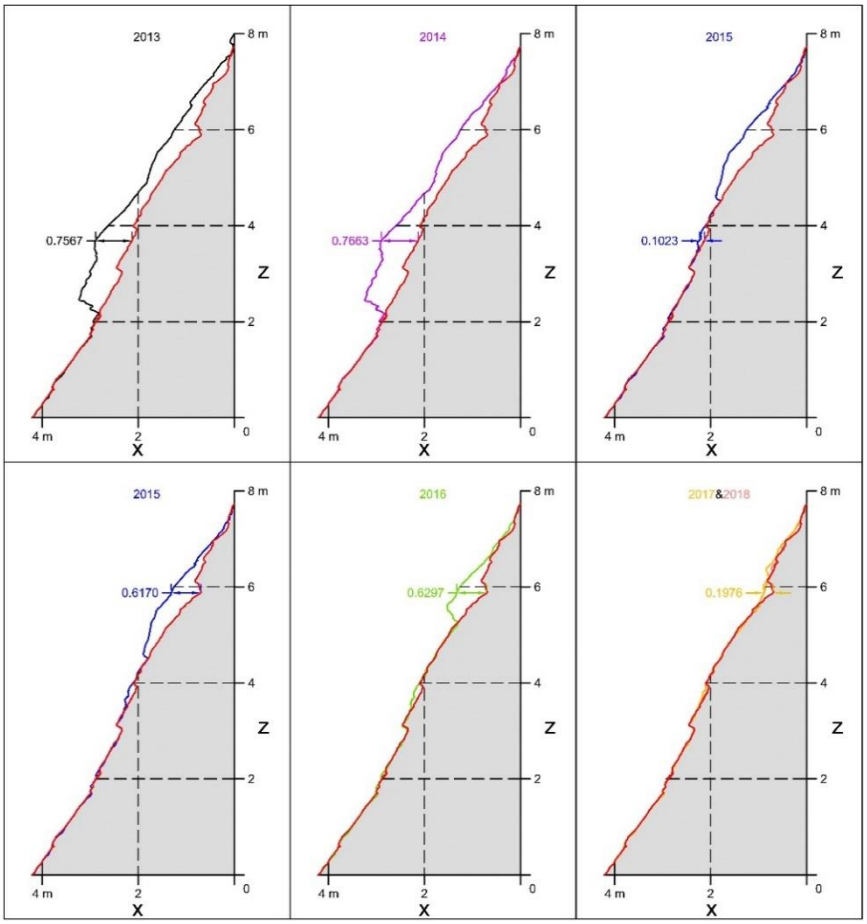

Figure 5. Cross-section for various monitoring epochs in reference to the 2019 cloud (red line).

The event itself is a minor detachment if approximately 0.1 m^3 and largest X-axis displacement of about 40 cm. It contributes little to the total rockfall product 2013-2019 (figure 4d), but its cross-section (figure 5d-e) suggest another important bulging in respect to 2016 sequence, equaling 0.0127 m (0.6297-0.6170 m) or 1.3 cm, which remains the upper threshold for pre-failure deformation in the sub-selected area.

In 2017 to 2018 there was practically no activity at this portion of the rock face (figure 3e, 4e), but comparison between 2018-2019 (figure 3f, 4f) is rather interesting. It surpasses the cross-sectional area (figure 5f) leaving no pre-failure thresholding example for the analysis, but it was evidently a wider event developed progressively, following a cluster of medium- to small-sized events of the preceding sequences. It partly encloses talus, but one medium-sized block of about 0.2 m^3 is missing in comparison to previous sequences. Its total contribution is redundant as it is the last comparison of sequences and its sequential detachments are in the same time its total detachments.

5. Conclusion

This work elaborates one medium-sized rockfall event (about 10 m^3 in total) and follows its progress on a roadside rock cut, during 2013-2019 period. TLS-based point clouds were produced for each year and cross-compared. The comparisons were performed between successive pairs of monitoring epochs, as well as in respect to the final situation, (2019). It is safe to conclude that the slope material exhibits expected detachment mechanism, which fits into the progressive failure along developing joint concept, while the general retreat of the fallen rock mass is expectedly in the upslope direction. The SSE-facing joint set (daylighting on the rock face) and E-facing set sever medium-sized blocks, undercut by the bedding plane (dipping into the mass), causing combined free-fall (more dominant) and rock-slide (subordinate, due to steep surfaces and insufficient friction) motion. Apart from regular large blocks,

there is also slope talus material that has been mobilized locally with blocks. It is also safe to conclude that pre-failure deformations can be routinely detected for larger blocks using proposed TLS monitoring program. Results are indicating that 1-1.3 cm displacements in direction opposite to X axis are a confident indicator for larger rockfall events, which by rule develop within the succeeding year, and appear as a missing mass in the following sequence point cloud. Given that the slope is regularly jointed by three sets, particularly by the one which is forming the face of the cut, all exhibited displacements can be observed in X axis, instead of using total vectors. Thus, the threshold displacement is not the total vector but its X component, which is more practical for systematic application of the approach. If applied systematically, it can provide excellent information for managing rockfall-prone slopes that have similar level of applicability of the TLS (static or mobile) approach as presented herein, possibly applicable not only on presented cut but also cuts in the same rock formation which are present in vicinity.

Acknowledgement
Supported by the Ministry of education, science and technological development of Serbia, TR36009.

References

[1] Erismann T and Abele G 2001 *Dynamics of Rockslides and Rockfalls* (Springer: Berlin) p 316
[2] Rosser N, Lim M, Petley D, Dunning S and Allison R 2007 Patterns of precursory rockfall prior to slope failure. *Jour. of Geoph. res.* **112** F04014.
[3] Abellán A, Calvet J, Vilaplana J M and Blanchard J 2010 Detection and spatial prediction of rockfalls by means of terrestrial laser scanner monitoring. *Geomorphology* **119** 162–171
[4] Kromer R A, Hutchinson D J, Lato M J, Gauthier D and Edwards T 2015 Identifying rock slope failure precursors using LiDAR for transportation corridor hazard management. Eng. Geol. **195** 93–103
[5] De Vilder S J, Rosser N J and Brain M J 2017 Forensic analysis of rockfall scars. *Geomorphology* **295** 202–214
[6] Janeras M, Jara J A, Royán M J, Vilaplana J M, Aguasca A, Fàbregas X, Gili J and Buxó P 2017 Multi-technique approach to rockfall monitoring in the Montserrat massif (Catalonia, NE Spain). *Eng. Geol.* **219** 4–20
[7] Marjanović M, Abolmasov B, Djurić U, Zečević S and Šušić V 2013 Basic kinematic analysis of a rock slope using terrestrial 3D laser scanning on the M-22 highroad pilot site. *Proc. of the EUROCK 2013*, 21-26 September, Wroslaw, Poland, pp 679-683
[8] Marjanović M, Đurić U, Abolmasov B and Bogdanović S 2014 Preliminary Analysis and Monitoring of the Rock Slope on the M-22 Highroad Near Ljig in Serbia, Using LiDAR Data. *Engineering Geology for Society and Territory - Landslide Processes*, *Vol. 2*: *Landslide Processes*, ed G Lollino et al. (Springer: Int.) pp. 147-150
[9] Bogdanović S, Marjanović M, Abolmasov B, Đurić U and Basarić I 2015 Rockfall Monitoring Based on Surface Models. *Surface Models for Geosciences*, ed K Růžičková, T Inspektor (Springer International Publishing: Int.) pp. 37-44
[10] Marjanović M, Abolmasov B, Pejić M, Bogdanović S and Samardžić-Petrović M 2017 Rockfall monitoring and simulation on a rock slope near Ljig in Serbia. *Proc. of the 3rd Reg. Symp. Landslides in the Adriatic Balkan Region*. 11-13 October, Slovenia, Ljubljana, pp 83-88
[11] Brodu N and Lague D 2012 3D Terrestrial LiDAR data classification of complex natural scenes using a multi-scale dimensionality criterion: applications in geomorphology. ISPRS jour. of Photogr. and Rem. Sens. **68** 121-134